A CONSERVATIVE DISCONTINUOUS GALERKIN METHOD FOR NONLINEAR ELECTROMAGNETIC SCHRÖDINGER EQUATIONS*

NIANYU YI†, YUNQING HUANG‡, AND HAILIANG LIU§

Abstract. Many problems in solid state physics and quantum chemistry require the solution of the Schrödinger equation in the presence of an electromagnetic field. In this paper, we construct, analyze, and numerically validate conservative discontinuous Galerkin (DG) schemes for the nonlinear magnetic Schrödinger equation. Both mass and energy conservation are shown for the semidiscrete DG scheme, and optimal L^2 error estimates are obtained in the full nonlinear setting. For the time discretization a second order Strang splitting is applied while mass is still conserved. A number of numerical tests are given to demonstrate the method's accuracy and robustness, and both mass and energy are well preserved over long time simulations.

Key words. DG methods, magnetic Schrödinger, BEC

AMS subject classifications. 35Q55, 65M15, 65M60

DOI. 10.1137/19M124229X

1. Introduction. Many problems in solid state physics and quantum chemistry require the solution of the Schrödinger equation in the presence of an electromagnetic field. The physical significance in such settings is particularly well known in nonlinear optics and Bose–Einstein condensate (BEC), where the magnetic structure is involved in scattering, superfluid, quantized vortices as well as the derivative nonlinear Schrödinger equation in plasma physics; see, e.g., [29, 8].

The aim of this paper is to design and analyze conservative discontinuous Galerkin (DG) schemes for the nonlinear Schrödinger (NLS) equation in the presence of an electromagnetic field, with particular attention on preservation of both mass and energy at the discrete level.

Our model equation is of the form

$$\text{(1.1)} \qquad \mathrm{i}u_t = -\frac{1}{2}\Delta_A u + \Phi(x)u + \mu|u|^{p-1}u,$$

where the unknown $u = u(x,t)$ is the quantum complex-valued wave function, $\Delta_A = \nabla_A^2$ with $\nabla_A = \nabla - \mathrm{i}A$, $\Phi : \mathbb{R}^d \to \mathbb{R}$ induces the electric field $-\nabla\Phi$, and $A = (A_1, \ldots, A_d)$ induces the magnetic field $\nabla \wedge A = (\partial_j A_i - \partial_i A_j)_{d \times d}$ with $d = 2, 3$. The linear operator $L = -\frac{1}{2}\Delta_A + \Phi$ is an essentially self-adjoint Schrödinger operator

---

†Hunan Key Laboratory for Computation and Simulation in Science and Engineering, School of Mathematics and Computational Science, Xiangtan University, Xiangtan 411105, People's Republic of China (yinianyu@xtu.edu.cn).

‡Corresponding author. Hunan Key Laboratory for Computation and Simulation in Science and Engineering, School of Mathematics and Computational Science, Xiangtan University, Xiangtan 411105, People's Republic of China (huangyq@xtu.edu.cn).

§Department of Mathematics, Iowa State University, Ames, IA 50011 (hliu@iastate.edu).

with an electromagnetic potential (Φ, A). The nonlinear term $F(u) = \mu|u|^{p-1}u$, where $1 < p < \infty$; the constant μ accounts for the attractive ($\mu < 0$) or repulsive ($\mu > 0$) interaction, whose sign depends on the chemical elements. Our results are mostly valid for general $F = g(|u|^2)u$, which has the property $\text{Im}(u^*F(u)) = 0$, where u^* is the complex conjugate of u.

The model problem has rich mathematical structures; for example, it is completely integrable when $p = 3$ and $\Phi = 0$, it has Hamiltonian structure, and the solution can blow up. The Hamiltonian $E = \int \frac{1}{2}|\nabla_A u|^2 + \Phi|u|^2 + \frac{2\mu}{p+1}|u|^{p+1}$ generates nonlinear system (1.1) by

$$(1.2) \qquad\qquad iu_t = \frac{1}{2}\frac{\delta E}{\delta u^*}.$$

When $p = 3$, we find the Gross–Pitaevskii equation (GPE), which is regarded as a Ginzburg–Landau model in string theory. The GPE describes the macroscopic wave functions u of the condensate in the presence of the electromagnetic potential (Φ, A). The nonlinear term results from the mean field interaction between atoms. Well-posedness for the initial value problem with L^2 data has been studied by several authors; see, e.g., [8, 27, 28, 38, 10].

In this work we set the boundary condition as either the periodic boundary condition or the homogeneous Dirichlet boundary condition

$$u(x, t) = 0, \quad x \in \partial\Omega.$$

With such boundary conditions and initial data $u(x, 0) = u_0(x)$, one can prove that both mass and energy remain conserved throughout its lifespan:

$$M(t) := \int_\Omega |u(x, t)|^2 dx = M(0),$$

$$E(t) := \int_\Omega \frac{1}{2}|\nabla_A u|^2 + \Phi|u|^2 + \frac{2\mu}{p+1}|u|^{p+1}dx = E(0).$$

When designing numerical methods, we would like our numerical approximations to respect the mass and energy conservation property, not only because it makes the numerical approximation physically meaningful, but also because it makes the numerical scheme more robust, since numerical methods without these properties may result in substantial shape errors after long time simulation. It is also desirable to observe numerical results that can experimentally verify the BEC theory and the magnetic effects.

In recent years, the DG schemes have been actively designed and applied for solving Schrödinger equations; see, e.g., [24, 33, 34, 35, 37, 25, 15, 36, 17, 13]. Xu and Shu [33] developed a local DG (LDG) method to solve the generalized NLS equation. For linearized Schrödinger equations, they proved the error estimate of order $k + 1/2$ for polynomials of degree k. The optimal error estimate was further proved in [34] by using special local projections. A mass-preserving LDG method was introduced in [24] for numerically solving linear Schrödinger equations. In contrast, mass-preserving DG schemes presented in [35, 37] are based on the direct DG (DDG) method, which was originally proposed by Liu and Yan [20, 21] for diffusion problems. For the LDG method to solve the two-dimensional NLS equation we refer the reader to [36], where the authors showed that the method can satisfy the discrete mass and energy conserving laws. Liang, Khaliq, and Xing [15] studied a mass-preserving LDG method

combined with the fourth order exponential time differencing Runge–Kutta method. Hong, Ji, and Liu [13] proposed a conservative LDG method with upwind-biased numerical fluxes. In [25], Lu, Huang, and Liu developed a high-order mass-conserving DG method to find numerical solutions for

$$(1.3) \qquad\qquad iu_t + \Delta u - |u|^2 u = 0.$$

A key observation in [25] is that the conservation property remains valid independent of the size of the penalty parameter. The optimal L^2 error estimate was also obtained in [25] for one-dimensional linear Schrödinger equations. An extension to the multidimensional setting was further carried out in [17], which presents two different approaches to handling both structured and unstructured meshes. For rectangular meshes, the error analysis is based on the tensor product of polynomials using the explicit projection constructed in [25], while a superconvergence result is used to recover the optimal L^2 error estimate. Moreover, the obtained result is valid with or without a flux parameter. For unstructured shape-regular meshes, the optimal error analysis is based on a global projection and its approximation error [3, 16]. The main advantage of such a method is its capacity to eliminate troublesome jump terms in the error equation, and it has been well applied to conservative DG methods for other dispersive PDEs—for instance, in [5] for the generalized KdV equation, in [18] for the Burgers–Poisson system, and in [19] on a Hamiltonian-preserving DG method to the generalized KdV equation.

   In this paper, we extend the ideas in [25, 17] to develop a novel conservative DG method to find numerical solutions for (1.1). The DG method is known to enjoy mathematically provable high-order accuracy and stability, and the discontinuous feature of its approximation space makes it a good fit for parallel implementation and for handling unstructured meshes; see, e.g., [12, 30, 31]. Our focus is on constructing a spatially high-order conservative DG scheme so that conservation properties are preserved even in the presence of both magnetic and electric fields.

   The main conclusion is that the semidiscrete schemes can preserve both mass and energy independent of the size of the flux parameter. Furthermore, the optimal L^2 error estimate is proved for nonlinear equation (1.1). For time discretization we follow our earlier work [25] in adopting the classical Strang splitting method [32], so that the resulting fully discrete scheme still preserves mass and is second order in time. Interested readers are referred to [4, 11, 26, 23, 14] for time splitting methods explored in solving the Schrödinger equation. In this paper, the proposed Strang splitting is realized by recording solution values only on quadrature points, and is hence inexpensive and easy to implement. It not only preserves the mass and high-order spatial accuracy but also makes the numerical scheme more robust.

   Finally, we should point out that splitting the magnetic Schrödinger equation for the purpose of its numerical solution into three subproblems has been explored by several authors; see, e.g., [14, 6], in which different semi-Lagrangian approaches are used for the solution of the advection step. In such a method mass is conserved only when A is divergence-free. Our treatment does not require such an assumption or use of the Coulomb gauge transformation to make it so. We remark that electric field $E = -\nabla\Phi - \partial_t A$ and magnetic field $H = \nabla \times A$ do not change at all under the transformation $u = Ue^{i\lambda}$ with A replaced by $A - \nabla\lambda$ and Φ replaced by $\Phi + \partial_t\lambda$; such gauge freedom may be used to simplify the model as needed—for instance, to make $\nabla \cdot A = 0$, which is called the Coulomb gauge.

   The remainder of the paper is organized as follows. In section 2, we start with the semidiscrete DG discretization of (1.1) for the problem with periodic or Dirichlet

boundary conditions, respectively; conservation properties for both mass and energy are further verified. Optimal L^2 error estimates are given in section 3. In section 4, we present the Strang splitting method for time discretization, which is shown to still preserve mass unconditionally. In section 5, we present numerical results to illustrate both focusing and defocusing nonlinear effects on the wave function of BEC subject to various anisotropic potentials, and the effects from the magnetic potentials. In particular, we study how well the considered numerical algorithms preserve mass and energy. Finally, concluding remarks are given in section 6.

Throughout this paper, we adopt standard notation for Sobolev spaces such as $W^{m,p}(D)$ on subdomain $D \subset \Omega$ equipped with the norm $\|\cdot\|_{m,p,D}$ and seminorm $|\cdot|_{m,p,D}$. When $D = \Omega$, we omit the index D; and if $p = 2$, we set $W^{m,p}(D) = H^m(D)$, $\|\cdot\|_{m,p,D} = \|\cdot\|_{m,D}$, and $|\cdot|_{m,p,D} = |\cdot|_{m,D}$. We also denote $\partial\Omega$ as the boundary of Ω. We use the notation $C \lesssim B$ to indicate that C can be bounded by B multiplied by a constant independent of the mesh size h. $C \sim B$ stands for $C \lesssim B$ and $B \lesssim C$. Also, we use $(\cdot)^+$ to denote $\max(\cdot, 0)$, and $(\cdot)^- = \min(\cdot, 0)$.

2. The direct DG method. We are interested in the high-order numerical approximation of the solution to (1.1) in multiple dimensions.

2.1. Scheme formulation. For simplicity, we assume the domain Ω to be a union of rectangular meshes
$$\Omega = \cup_{\alpha=1}^N K_\alpha,$$
where $\alpha = (\alpha_1, \ldots, \alpha_d)$, $N = (N_1, \ldots, N_d)$. We use rectangular meshes $\{K\} \subset \mathcal{T}_h$, with $K_\alpha = I_{\alpha_1}^1 \times \cdots \times I_{\alpha_d}^d$, where $I_{\alpha_i}^i = [x_{\alpha_i-1/2}^i, x_{\alpha_i+1/2}^i]$ for $\alpha_i = 1, \ldots, N_i$. Denote $h_i = \max_{1 \le \alpha_i \le N_i} |I_{\alpha_i}^i|$, with $h = \max_{1 \le i \le d} h_i$.

We define the DG space as the space of tensor products of piecewise polynomials of degree at most k in each variable on every element, i.e.,
$$V_h = \{v : v \in Q^k(K_\alpha), \quad \alpha = 1, \ldots, N\},$$
where Q^k is the space of tensor products of one-dimensional polynomials of degree up to k. For the one-dimensional case, we have $Q^k(K) = P^k(K)$, which is the space of polynomials of degree at most k defined on K. Hence the traces of functions in V_h are double-valued on $\Gamma_h^0 := \Gamma_h \backslash \partial\Omega$ and single-valued on $\Gamma_h^\partial = \partial\Omega$, where $\Gamma_h = \Gamma_h^0 \cup \Gamma_h^\partial$.

We also introduce some trace operators that will help us to define the interface terms. Let K^1 and K^2 be two neighboring cells with a common edge e; for w defined on ∂K^i, $i = 1, 2$, we define the average $\{w\}$ and the jump $[w]$ as follows:
$$\{w\} = \frac{1}{2}(w_1 + w_2), \quad [w] = w_2 - w_1 \quad \text{on} \quad e = \bar{K}_1 \cap \bar{K}_2,$$
where the jump is calculated as a forward difference along the normal direction n, which is defined to be oriented from K^1 to K^2, with $w_i = w|_{\partial K^i}$.

Note that
$$\Delta_A u = \nabla \cdot (\nabla u - 2iAu) + (i\nabla \cdot A - |A|^2)u.$$
Let v^* denote the complex conjugate of v, and let the inner product be defined as
$$\langle u, v \rangle_K = \int_\Omega uv^* dx, \qquad \langle u, v \rangle_{\partial K} = \int_{\partial K} uv^* ds.$$
First we apply the DG approximation to $\int_K \Delta_A uv^* dx$ on each element $K \in \mathcal{T}_h$ to obtain
$$\langle \Delta_A u, v \rangle_K \sim -\langle (\nabla - 2iA)u_h, \nabla v \rangle_K + \langle (i\nabla \cdot A - |A|^2)u_h, v \rangle_K$$

$$+ \langle \widehat{\partial_n u_h} - 2\mathrm{i} A \cdot n \widetilde{u_h}, v \rangle_{\partial K} + \langle u_h - \widehat{u_h}, \partial_n v \rangle_{\partial K} \quad \forall u_h, v \in V_h,$$

with the numerical fluxes taken as

$$(2.1) \qquad \widehat{\partial_n u_h} = \beta h_e^{-1} [u_h] + \{\partial_n u_h\}, \quad \widehat{u_h} = \widetilde{u_h} = \{u_h\},$$

where, on the interface with $x^i = x^i_{\alpha_i + 1/2}$,

$$h_e = \frac{1}{2}(|I^i_{\alpha_i}| + |I^i_{\alpha_{i+1}}|).$$

Note that for uniform meshes we have $h_e = h_i$. These numerical fluxes are single-valued on the edge of element K as the approximation of $\partial_n u$. The choice of parameter β will be discussed later.

Note that for $\partial K \in \Gamma_h^\partial$, when subject to a homogeneous boundary condition, we choose

$$(2.2) \qquad \widehat{u_h} = 0, \quad \widetilde{u_h} = u_h/2,$$

$$(2.3) \qquad \widehat{\partial_n u_h} = -\beta h_e^{-1} u_h + \partial_n u_h.$$

With this we have the DG scheme

$$(2.4) \qquad \mathrm{i} \int_\Omega u_{ht} v^* dx = \frac{1}{2} B_A(u_h, v) + \int_\Omega \left(\Phi(x) + \mu |u_h|^{p-1} \right) u_h v^* dx,$$

where the bilinear functional

$$B_A(u_h, v) = B_A^0(u_h, v) + B_A^b(u_h, v)$$

with

$$B_A^0(u_h, v) = \sum_{K \in \mathcal{T}_h} \left(\langle \nabla u_h - 2\mathrm{i} A u_h, \nabla v \rangle_K - \langle (\mathrm{i} \nabla \cdot A - |A|^2) u_h, v \rangle_K \right)$$

$$(2.5) \qquad + \sum_{e \in \Gamma_h^0} \langle \widehat{\partial_n u_h} - 2\mathrm{i} A \cdot n \{u_h\}, [v] \rangle_e + \langle [u_h], \{\partial_n v\} \rangle_e,$$

and $B_A^b(u_h, v)$ is given below for each respective type of boundary condition:

(2.6a)

$$\text{for periodic case } B_A^b(u_h, v) = \frac{1}{2} \int_{\partial \Omega} (\widehat{\partial_n u_h} - 2\mathrm{i} A \cdot n u_h)[v^*] + [u_h]\{\partial_n v^*\} ds,$$

(2.6b)

$$\text{for Dirichlet condition } B_A^b(u_h, v) = \int_{\partial \Omega} ((\beta h_e^{-1} u_h - \partial_n u_h + \mathrm{i} A \cdot n u_h)v^* - u_h \partial_n v^*) ds.$$

Note that the factor $1/2$ in (2.6a) is used to indicate that for the periodic boundary condition only one end in the x_i direction should be counted. Here $h_e = h_i$ at each interface $x^i_{\alpha^i + 1/2}$ for $\alpha_i = 1, \ldots, N_i$. Note that in formulation (2.5) the choice of n on the edge $e \in \Gamma_h^0$ (pointing to K_1 or K_2) does not affect the products $A \cdot n\{u_h\}[v^*]$, $\widehat{\partial_n u_h}[v^*]$, and $[u_h]\{\partial_n v^*\}$. Hence both $\{\partial_n u\}$ and $\{\partial_n v\}$ are defined based on a fixed choice of n on e. However, on $e \in \Gamma_h^\partial$, n is taken as the usual outside normal unit to $\partial \Omega \cap e$.

The initial data for the obtained semidiscrete DG scheme is given as

$$u_h(x, 0) = \Pi u_0,$$

where Π is the standard piecewise L_2 projection.

2.2. Conservation properties. In order to establish the conservation properties of the scheme, we prepare the following lemma.

LEMMA 2.1. *Let a, b be complex polynomials in V_h; then*

$$B_A(a, b) = \overline{B_A(b, a)}. \tag{2.7}$$

Proof. We verify this for the case with Dirichlet boundary data. The periodic case is even simpler, and so details are omitted. Note that

$$
\begin{aligned}
B_A(a, b) = &\sum_{K \in \mathcal{T}_h} \int_K ((\nabla a - 2\mathrm{i}Aa) \cdot \nabla b^* + (-\mathrm{i}\nabla \cdot A + |A|^2)ab^*)dx \\
&+ \sum_{e \in \Gamma_h^0} \int_e \left((\beta h_e^{-1}[a] + \{\partial_n a\} - 2\mathrm{i}A \cdot n\{a\})[b^*] + [a]\{\partial_n b^*\} \right) ds \\
&+ \int_{\partial\Omega} \left((\beta h_e^{-1}a - \partial_n a + \mathrm{i}A \cdot na)b^* - a\partial_n b^* \right) ds.
\end{aligned}
$$

This allows us to evaluate

$$
\begin{aligned}
B_A(a, b) - \overline{B_A(b, a)} = &\sum_{K \in \mathcal{T}_h} \int_K (-2\mathrm{i}A \cdot \nabla b^* a - 2\mathrm{i}A \cdot \nabla a b^* - 2\mathrm{i}\nabla \cdot A(ab^*))dx \\
&+ \sum_{e \in \Gamma_h^0} \int_e (-2\mathrm{i}A \cdot n(\{a\}[b^*] + \{b^*\}[a])) ds + \int_{\partial\Omega} (2\mathrm{i}A \cdot nab^*) ds \\
&= -2i \left[\sum_{K \in \mathcal{T}_h} \int_K \nabla \cdot (Aab^*)dx + \sum_{e \in \Gamma_h^0} \int_e A \cdot n[ab^*]ds - \int_{\partial\Omega} A \cdot nab^* ds \right] \\
&= 0,
\end{aligned}
$$

as desired. $\square$

Denote

$$\|v\|_E^2 := \sum_{K \in \mathcal{T}_h} \|\nabla_A v\|_K^2 + \sum_{e \in \Gamma_h} h_e^{-1}|[v]|_e^2. \tag{2.8}$$

For the semidiscrete DG scheme (2.4), we have the following conservation property for both mass and energy at the discrete level.

THEOREM 2.1. *The semidiscrete DG scheme (2.4) for any $\beta \in \mathbb{R}$ satisfies two discrete conservation laws:*

$$
\begin{aligned}
M_h(t) &:= \int_\Omega |u_h(x, t)|^2 dx = M_h(0), \\
E_h(t) &:= \frac{1}{2}B_A(u_h, u_h) + \int_\Omega \left(\Phi|u_h|^2 + \frac{2\mu}{p+1}|u_h|^{p+1} \right) dx = E_h(0).
\end{aligned}
$$

Furthermore, there exist $\Gamma > 0$ and $\alpha \in (0, 1)$ such that if $\beta > \Gamma$, then

$$B_A(v, v) \geq \alpha\|v\|_E^2. \tag{2.9}$$

Proof. Take $v = u_h$ in (2.4) to obtain

$$\mathrm{i}\int_\Omega u_{ht}u_h^* dx = \frac{1}{2}B_A(u_h, u_h) + \int_\Omega \left(\Phi(x) + \mu|u_h|^{p-1} \right) |u_h|^2 dx.$$

Hence, using (2.7), we have

$$\frac{d}{dt}\|u_h\|^2 = \frac{1}{2i}\left(B_A(u_h, u_h) - \overline{B_A(u_h, u_h)}\right) = 0.$$

Furthermore, we choose $v = u_{ht}$ in (2.4), so that

$$i\int_\Omega |u_{ht}|^2 dx = \frac{1}{2}B_A(u_h, u_{ht}) + \int_\Omega \left(\Phi(x) + \mu|u_h|^{p-1}\right)u_h u_{ht}^* dx.$$

This upon adding its conjugate gives

$$\frac{d}{dt}\left(\frac{1}{2}B_A(u_h, u_h) + \int_\Omega \Phi|u_h|^2 + \frac{\mu}{p+1}|u_h|^{p+1}\right) = J,$$

where, by (2.7),

$$J = \frac{1}{2}\left(B_A(u_{ht}, u_h^*) - \overline{B_A(u_h, u_{ht}^*)}\right) = 0.$$

Finally we show (2.9). Regrouping terms, we rewrite

$$\begin{aligned}
B_A(v, v) &= \sum_{K\in\mathcal{T}_h}\int_K (|\nabla v|^2 - 2i(A\cdot\nabla)v^* v - (i\nabla\cdot A - |A|^2)|v|^2)dx \\
&\quad + \sum_{e\in\Gamma_h^0}\int_e \left(\beta h_e^{-1}|[v]|^2 + \{\partial_n v\}[v^*] + [v]\{\partial_n v^*\} - 2iA\cdot n\{v\}[v^*]\right)ds \\
&\quad + \int_{\partial\Omega}\left(\beta h_e^{-1}|v|^2 - \partial_n vv^* - v\partial_n v^* + iA\cdot nvv^*\right)ds \\
&= \sum_{K\in\mathcal{T}_h}\int_K |\nabla_A v|^2 dx + \int_{\partial\Omega}\left(\beta h_e^{-1}|v|^2 - \partial_n vv^* - v\partial_n v^*\right)ds \\
&\quad + \sum_{e\in\Gamma_h^0}\int_e \left(\beta h_e^{-1}|[v]|^2 + \{n\cdot\nabla_A v\}[v^*] + [v]\{n\cdot\overline{\nabla_A v}\}\right)ds.
\end{aligned}$$

Further, with the notation $\partial_A = n\cdot\nabla_A$, we have

$$\begin{aligned}
B_A(v, v) &= \sum_{K\in\mathcal{T}_h}\int_K |\nabla_A v|^2 dx + \sum_{e\in\Gamma_h}\frac{\beta}{h_e}\int_e |[v]|^2 ds + 2\sum_{e\in\Gamma_h} Re\int_e (\{\partial_A v\}[v^*])ds \\
&\geq \sum_{K\in\mathcal{T}_h}\int_K |\nabla_A v|^2 dx + \sum_{e\in\Gamma_h}\frac{\beta}{h_e}\int_e |[v]|^2 ds - \left(\sum_{e\in\Gamma_h}\int_e |\{\partial_A v\}|^2 ds\right)^{1/2}\left(\sum_{e\in\Gamma_h}\int_e |[v]|^2 ds\right)^{1/2} \\
&\geq \sum_{K\in\mathcal{T}_h}\int_K |\nabla_A v|^2 dx - \frac{\epsilon}{2}\sum_{e\in\Gamma_h} h_e\int_e |\{\partial_A v\}|^2 ds + \left(\beta - \frac{1}{2}\epsilon^{-1}\right)\sum_{e\in\Gamma_h} h_e^{-1}\int_e |[v]|^2 ds.
\end{aligned}$$

Set

$$(2.10) \qquad \Gamma \geq \frac{1}{4}\sup_{v\in V_h}\frac{\sum_{e\in\Gamma_h} h_e\int_e |\{\partial_A v\}|^2 ds}{\sum_{K\in\mathcal{T}_h}\int_K |\nabla_A v|^2 dx}.$$

We have
(2.11)
$$B_A(v, v) \geq (1 - 2\epsilon\Gamma)\sum_{K\in\mathcal{T}_h}\int_K |\nabla_A v|^2 dx + \left(1 - \frac{1}{2\beta\epsilon}\right)\sum_{e\in\Gamma_h}\beta h_e^{-1}\int_e |[v]|^2 ds \geq \alpha\|v\|_E^2,$$

where $\alpha = (1 - 2\epsilon\Gamma)\min\{1, \beta\}$ with

$$1 - 2\epsilon\Gamma = 1 - \frac{1}{2\beta\epsilon} = 1 - \sqrt{\frac{\Gamma}{\beta}} > 0,$$

provided $\epsilon = \frac{1}{2}(\Gamma\beta)^{-1/2}$ and $\beta > \Gamma$. This completes the proof. $\qquad\square$

Remark 2.1. The condition $\beta > \Gamma$ with Γ implicitly given is only a sufficient condition. In most cases of our numerical tests, β can be chosen as zero or a small fixed number.

3. Optimal L^2 error estimates. In this section, we derive the optimal error estimates for the conservative DDG method proposed in section 2.1 for

$$(3.1) \qquad\qquad iu_t = -\frac{1}{2}\Delta_A u + \Phi(x)u + \mu|u|^{p-1}u.$$

We will give error estimates in the L^2 norm for this model with periodic boundary condition. Error estimates with other boundary conditions can be obtained as well in a similar fashion; details are omitted.

For $v \in V = V_h + H^2(\Omega)$, we define the DG norm as

$$(3.2) \qquad \|v\|^2 = \sum_{K \in \mathcal{T}_h} \|\nabla_A v\|_K^2 + \sum_{K \in \mathcal{T}_h} h_K^2 |v|_{2,K}^2 + \sum_{e \in \Gamma_h} h_e^{-1} |[v]|_e^2,$$

where h_e is the characteristic length of the edge e. One can verify that

$$(3.3) \qquad\qquad |B_A(w, v)| \leq \Lambda \|w\| \cdot \|v\| \quad \forall w, v \in V,$$

where Λ is called the continuous constant. Furthermore, for $v \in V_h$, we have

$$(3.4) \qquad\qquad \|v\|_E^2 \leq \|v\|^2 \leq C_0 \|v\|_E^2$$

for a constant $C_0 > 1$. Actually we can show this using the following fact.

LEMMA 3.1. *There exists $C > 0$ such that*

$$(3.5) \qquad\qquad \|\nabla v\|_K^2 \leq C \|\nabla_A v\|_K^2 \quad \forall v \in V_h.$$

Proof. It suffices to show that if $\nabla v - iAv = 0$, then $v = 0$ for $v \in V_h$. To see this, let $v = a + ib$, with a and b real polynomials in V_h. From $\nabla v - iAv = 0$, we obtain

$$\begin{cases} \nabla a = -Ab, \\ \nabla b = Aa. \end{cases}$$

Then

$$\frac{1}{2}\nabla(a^2 + b^2) = a\nabla a + b\nabla b = -Aba + Aab = 0,$$

which yields

$$a^2 + b^2 \equiv \text{const}.$$

Hence $a = 0$ and $b = 0$. Noticing that $\nabla v = \nabla_A v + iAV$, we obtain

$$\|\nabla v\|_K^2 \leq 2\|\nabla_A v\|_K^2 + 2\|Av\|_K^2 \leq C\|\nabla_A v\|_K^2. \qquad\qquad \square$$

3.1. Projection and approximation properties. We first introduce a projection and then present its approximation properties. Define the projection Π of a function w into space V_h as follows:

$$(3.6) \qquad \int_\Omega (w - \Pi w) v^* dx + B_A(w - \Pi w, v) = 0 \qquad \forall v \in V_h.$$

This projection is uniquely defined; since for $w = 0$ with $v = -\Pi w$ we have

$$0 = \|v\|^2 + B_A(v, v) \geq \|v\|^2 + \alpha \|v\|_E^2 \qquad \forall v \in V_h,$$

where we have used the coercivity (2.9), and hence $v \equiv 0$. This says that such a projection is well defined.

THEOREM 3.1. *For $w \in H^{k+1}$ and h suitably small, we have the following projection error:*

$$(3.7) \qquad \|w - \Pi w\| \leq Ch^{k+1} |w|_{k+1} \ \text{and} \ \|w - \Pi w\| \leq Ch^k |w|_{k+1},$$

where C depends on k, d, $1/\alpha$, and Λ.

Proof. We carry out the proof in two steps.

Step 1. We first bound the projection error $R := w - \Pi w$ in the following way: for any $v \in V_h$, we have

$$
\begin{aligned}
C_0^{-1} \alpha \|v - \Pi w\|^2 \leq \alpha \|v - \Pi w\|_E^2 &\leq B_A(v - \Pi w, v - \Pi w) \\
&= B_A(v - w, v - \Pi w) + \int_\Omega (\Pi w - w)(v - \Pi w)^* dx \\
&\leq \Lambda \|v - w\| \cdot \|v - \Pi w\| + \|R\| \cdot \|v - \Pi w\|.
\end{aligned}
$$

By this and the triangle inequality we obtain

$$
\begin{aligned}
\|R\|^2 &\leq 2 \inf_{v \in V_h} \left(\|v - w\|^2 + \|v - \Pi w\|^2 \right) \\
&\leq C \inf_{v \in V_h} \left(\|v - w\|^2 + \|v - w\| \cdot \|v - \Pi w\| + \|R\| \cdot \|v - \Pi w\| \right) \\
&\leq C \left(\|Qw - w\|^2 + \|Qw - w\| \cdot \|Qw - \Pi w\| + \|R\| \cdot \|Qw - \Pi w\| \right),
\end{aligned}
$$

where $C = 2 \max\{1, C_0 \Lambda / \alpha, C_0 / \alpha\}$. Here we have taken $v = Qw \in V_h$ to be the usual interpolant polynomial such that

$$\|\partial_x^m (w - Qw)\|_K \leq Ch_K^{k+1-m} |w|_{k+1,K},$$

where C depends on k, d; see [7].

This when combined with the estimate

$$|w|_{0,\partial K}^2 \leq C(h_K^{-1} |w|_{0,K}^2 + h_K |w|_{1,K}^2)$$

yields

$$(3.8) \qquad \|w - Qw\|^2 \leq Ch^{2k} |w|_{k+1,\Omega}^2.$$

Therefore,

$$\|R\|^2 \leq C(h^{2k} |w|_{k+1}^2 + h^k |w|_{k+1} \|R\| + h^{k+1} |w|_{k+1} \|R\| + \|R\|^2)$$

$$\leq (C+1/2)h^{2k}|w|_{k+1}^2 + \frac{1}{2}\|R\|^2 + \frac{C}{2}h^{2k+2}|w|_{k+1}^2 + \frac{3C}{2}\|R\|^2.$$

Hence

$$(3.9) \qquad \|R\|^2 \leq (1 + 2C + Ch^2)h^{2k}|w|_{k+1}^2 + 3C\|R\|^2.$$

Step 2. We proceed to obtain $\|R\|$ by coupling with a duality argument. Define the auxiliary function ψ as the solution of the adjoint problem

$$(3.10) \qquad \begin{cases} \psi - \Delta_A \psi = R & \text{in } \Omega, \\ \psi \text{ satisfies the periodic boundary condition on } \partial\Omega. \end{cases}$$

This problem has a unique solution and admits the following regularity estimate for $\psi \in H^2(\Omega)$:

$$(3.11) \qquad \|\psi\|_2 \leq \|R\|.$$

We then have
(3.12)
$$\|R\|^2 = \sum_{K \in \mathcal{T}_h} \int_K R^*(\psi - \Delta_A \psi)dx$$
$$= \sum_{K \in \mathcal{T}_h} \int_K R^*\psi dx + \sum_{K \in \mathcal{T}_h} \int_K (\nabla R^* \cdot \nabla \psi - 2iA \cdot \nabla R^* \psi + (|A|^2 - i\nabla \cdot A)R^*\psi)dx$$
$$\quad + \sum_{K \in \mathcal{T}_h} \int_{\partial K} \left(-R^* \frac{\partial \psi}{\partial n} + 2iA \cdot n R^*\psi \right) ds$$
$$= \sum_{K \in \mathcal{T}_h} \int_K R^*\psi dx + \sum_{K \in \mathcal{T}_h} \int_K (\nabla R^* \cdot \nabla \psi - 2iA \cdot \nabla R^* \psi + (|A|^2 - i\nabla \cdot A)R^*\psi)dx$$
$$\quad + \sum_{e \in \Gamma_h} \int_e \left(\frac{\beta}{h_e} \int_e [R^*][\psi] + \{\partial_n R^*\}[\psi] - 2iA \cdot n[R^*]\{\psi\} + [R^*]\{\partial_n \psi\} \right) ds$$
$$= \int_\Omega R^*\psi dx + B_A(\psi, R)$$
$$= \int_\Omega R\psi^* dx + B_A(R, \psi).$$

For $k \geq 1$, we take $\psi_h \in V_h$ to be a piecewise linear interpolant of ψ so that

$$\|\partial_x^m(\psi - \psi_h)\| \leq Ch^{2-m}|\psi|_2, \quad m = 0, 1, 2.$$

From (3.6) it follows that $\int_\Omega Rv dx + B_A(R, v) = 0$ for any $v \in V_h$. Using this formula with $v = \psi_h$, we obtain

$$\|R\|^2 = \int_\Omega R\psi^* dx + B_A(R, \psi) = \int_\Omega R(\psi^* - \psi_h^*)dx + B_A(R, \psi - \psi_h)$$
$$(3.13) \qquad \leq \|R\| \cdot \|\psi - \psi_h\| + \Lambda\|R\| \cdot \|\psi - \psi_h\|$$
$$\leq Ch^2|\psi|_2\|R\| + Ch|\psi|_2\|R\|$$
$$\leq C(h^2\|R\| + h\|R\|)\|R\|,$$

where we have used (3.11). Hence

$$(3.14) \qquad \|R\| \leq Ch(h\|R\| + \|R\|).$$

For $h \leq 1/\sqrt{2C}$, (3.14) yields

$$\|R\| \leq \frac{Ch}{1 - Ch^2}\|R\| \leq 2Ch\|R\|.$$

This upon substitution into (3.9) gives

$$(1 - 12C^3h^2)\|R\|^2 \leq (1 + 2C + Ch^2)h^{2k}|w|_{k+1}^2.$$

Further taking $h^2 \leq \frac{1}{24C^3}$ we have

$$\|R\|^2 \leq (3 + 4C)h^{2k}|w|_{k+1}^2.$$

Hence, for h suitably small,

$$\|R\| \leq Ch^{k+1}|w|_{k+1} \text{ and } \|R\| \leq Ch^k|w|_{k+1}.$$

The proof is now complete.   □

We collect a few very basic inequalities, in which the bounding coefficients are easy to figure out in one dimension, yet often more involved in the case of several dimensions.

(1) Note that if $w \in H^3(K)$ and e is an edge of element K, we have [2, (2.4) and (2.5)] the following trace inequalities:

$$(3.15a) \qquad \|v\|_{0,e}^2 \leq C(h_e^{-1}\|v\|_{0,K}^2 + h_e|v|_{1,K}^2),$$
$$(3.15b) \qquad \|\partial_n v\|_{0,e}^2 \leq C(h_e^{-1}|v|_{1,K}^2 + h_e|v|_{2,K}^2),$$
$$(3.15c) \qquad \|\partial_n^2 v\|_{0,e}^2 \leq C(h_e^{-1}|v|_{2,K}^2 + h_e|v|_{3,K}^2),$$

where the constant C can depend on several geometric features of K, but it does not depend on the size of K and e.

(2) Inverse inequality. In a finite dimensional space, all norms are equivalent. For every polynomial of degree $\leq k$, there exists C depending on k such that

$$(3.16) \qquad |v|_{s,K}^2 \leq Ch_K^{-2(s-m)}|v|_{m,K}^2 \quad \text{for } s, m \text{ integers with } s > m.$$

Moreover, for any function $v \in V_h$, the following inverse inequalities hold:

$$(3.17a) \qquad \|v\|_{\Gamma_h} \leq Ch^{-1/2}\|v\|,$$
$$(3.17b) \qquad \|v\|_\infty \leq Ch^{-d/2}\|v\|,$$

where d is the spatial dimension, and $\|v\|_{\Gamma_h}^2 := \sum_{e \in \Gamma_h} \int_e v^2 ds$. For more details of these inverse properties, we refer the reader to [7].

3.2. Error estimates. In order to obtain the error estimates for solutions to the mass-conserving DG scheme, we first give the error equations. Notice that this DG scheme is also satisfied when the numerical solution u_h is replaced by the exact solutions u (due to consistency of the DG method). The error equation becomes

$$(3.18) \qquad i\int_\Omega (u_t - u_{ht})v^* dx = \frac{1}{2}B_A(u - u_h, v) + \int_\Omega \Phi(u - u_h)v^* dx + H[v]$$

for all $v \in V_h$. Here

$$H[v] := \mu \int_\Omega (|u|^{p-1}u - |u_h|^{p-1}u_h)v^* dx.$$

Set $\xi = \Pi u - u, \eta = \Pi u - u_h$, and $v = \eta$; we have

$$(3.19) \quad \mathrm{i} \int_\Omega \eta_t \eta^* dx = \mathrm{i} \int_\Omega \xi_t \eta^* dx + \frac{1}{2}B_A(\eta, \eta) - \frac{1}{2}B_A(\xi, \eta) + \int_\Omega \Phi(\eta - \xi)\eta^* dx + H[\eta].$$

Thus

$$(3.20) \quad \frac{d}{dt}\|\eta\|^2 = 2\mathrm{Re}\left(\int_\Omega \xi_t \eta^* dx\right) - \mathrm{Im}(B_A(\xi, \eta)) - 2\mathrm{Im}\left(\int_\Omega \Phi\xi\eta^* dx\right) - 2\mathrm{Im}H[\eta].$$

Note that $B_A(\xi, \eta) = -\int_\Omega \xi\eta^* dx$, and the first three terms on the right are bounded from above by
(3.21)
$$2\|\xi_t\|\cdot\|\eta\| + 2\|\xi\|\cdot\|\eta\| + 2\|\Phi\|_\infty\|\xi\|\cdot\|\eta\| \le (2\|\xi_t\| + 2\|\xi\| + 2\|\Phi\|_\infty\|\xi\|)\|\eta\| \le Ch^{k+1}\|\eta\|,$$

where C depends on $|u|_{k+1}, |u_t|_{k+1}$, and $\|\Phi\|_\infty$. We proceed to estimate the nonlinear term as follows:

$$\begin{aligned}
2|H[\eta]| &= 2\mu\left|\int_\Omega \left(\int_0^1 \frac{d}{ds}\left(|u_s|^{p-1}u_s\right)ds\right)\eta^* dx\right| \qquad (u_s := su + (1-s)u_h)\\
&= 2\mu\left|\int_\Omega \int_0^1 p|u_s|^{p-1}(u - u_h)\eta^* ds dx\right|\\
&\le 2\mu p\left|\int_\Omega \int_0^1 |su + (1-s)u_h|^{p-1}|u - u_h||\eta^*| ds dx\right|\\
&= 2\mu p\left|\int_\Omega |u + (1-s^*)(\xi - \eta)|^{p-1}|\xi - \eta||\eta| dx\right| \qquad (s^* \in (0, 1))\\
&\le 2\mu p\|u + (1-s^*)(\xi - \eta)\|_\infty^{p-1}\int_\Omega |\eta - \xi||\eta| dx\\
&\le 2^p\mu p(\|u\|_\infty^{p-1} + \|\xi - \eta\|_\infty^{p-1})(\|\eta\| + \|\xi\|)\|\eta\|.
\end{aligned}$$

Using the Sobolev embedding result, we have for $k > \frac{d}{2} - 1$

$$\|u\|_\infty \le C\|u\|_{k+1}.$$

Using the approximation results (3.7), we have for small h

$$\|\xi - \eta\|_\infty \le \|\xi\|_\infty + \|\eta\|_\infty \le C(h^k + h^{-d/2}\|\eta\|),$$

where we have used (3.17b) and the following fact:

$$\begin{aligned}
\|\xi\|_\infty &\le \|u - u_I\|_\infty + \|u_I - \Pi u\|_\infty\\
&\le C(h^k + h^{-1}\|u_I - \Pi u\|)\\
&\le Ch^k,
\end{aligned}$$

where u_I is a local interpolation polynomial to approximate u. Hence (3.20) reduces to

$$\frac{d}{dt}\|\eta\|^2 \le Ch^{k+1}\|\eta\| + C^{p-1}2^{2p-1}\mu p(\|u\|_{k+1}^{p-1} + h^{-(p-1)d/2}\|\eta\|^{p-1} + h^k)(\|\eta\| + h^{k+1})\|\eta\|.$$

Set $B = \frac{\|\eta\|}{h^{k+1}}$, so that for $h < 1$,

$$\epsilon = h^{(k+1-d/2)(p-1)} < 1,$$

and we have

(3.22)
$$\frac{d}{dt}B \leq C(\epsilon B^{p-1} + 1)(B + 1),$$

where $h^{k+1-d/2} < 1$ has been used. Note that at $t = 0$ we have

$$\eta(x, 0) = \Pi u_0(x) - u_h(x, 0) = \xi(x; 0) + u_0(x) - u_h(x, 0);$$

hence $\|\eta(\cdot, 0)\|^2 \leq C_1 h^{2k+2}$ by (3.7) and the L^2-projection error, with C_1 depending on $\|u_0\|_{k+1}$. Thus $B(0) = \|\eta(\cdot, 0)\|/h^{k+1} \leq C_1$.

Integration of (3.22) gives

$$G(B(t)) \leq G(B(0)) + CT, \quad G(s) := \int_1^s \frac{dz}{(\epsilon z^{p-1} + 1)(z + 1)}$$

for $t \in [0, T]$. If $B(t) \leq 1$, then the proof is done. Otherwise, for $B(t) > 1$, we bound G from below as follows:

$$\begin{aligned}
G(B) &\geq \frac{1}{2} \int_1^B \frac{dz}{z(1 + \epsilon z^{p-1})} \\
&= \frac{1}{2} \int_{\epsilon^{\frac{1}{p-1}}}^{B\epsilon^{\frac{1}{p-1}}} \frac{dy}{y(1 + y^{p-1})} \qquad (\text{set } \epsilon z^{p-1} = y^{p-1}) \\
&= \frac{1}{2(1-p)} \log(1 + B^{1-p}/\epsilon) - \frac{1}{2(1-p)} \log(1 + 1/\epsilon).
\end{aligned}$$

Hence we have

$$\frac{1}{2(1-p)} \log(1 + B^{1-p}/\epsilon) - \frac{1}{2(1-p)} \log(1 + 1/\epsilon) \leq G(B(0)) + CT,$$

from which we are able to derive

$$B(t) \leq \left[\frac{e^a}{1 - \epsilon(e^a - 1)}\right]^{\frac{1}{p-1}}, \quad a = 2(p-1)(G(B_0) + CT).$$

It suffices to choose h suitably small so that $\epsilon \leq \frac{1}{2(e^a-1)}$, and as a result we have

$$B(t) \leq [2e^a]^{\frac{1}{p-1}} = 2^{\frac{1}{p-1}} e^{2(G(B_0)+CT)} = C^*.$$

We thus conclude $B(t) \leq \max\{1, C^*\}$. Hence $\|\eta(\cdot, t)\| \leq \max\{1, C^*\}h^{k+1}$, which when combined with the triangle inequality $\|u(\cdot, t) - u_h(\cdot, t)\| \leq \|\eta\| + \|\xi\|$ leads to the desired error estimate.

The main result can now be summarized as follows.

THEOREM 3.2. *Let u_h be the solution to the semidiscrete DG scheme* (2.4), (2.5) *with $\beta > \Gamma$, which depends on degree k of polynomial elements, and let u be the smooth solution of* (3.1) *subject to periodic boundary conditions. If $k > d/2 - 1$ and h is suitably small, then we have the following error estimate:*

$$\|u(\cdot, t) - u_h(\cdot, t)\| \leq Ch^{k+1}, \qquad 0 \leq t \leq T,$$

where C depends on $|u|_{k+1}, |u_t|_{k+1}, \|\Phi\|_\infty, T, \beta,$ and $\|u_0\|_{k+1}$ but is independent of h.

Remark 3.1. The above results can be generalized to the case with other boundary conditions. For example, for the Dirichlet boundary condition with $u(x,t) = 0$ for $x \in \partial\Omega$, the corresponding DG scheme becomes

$$\mathrm{i}\int_\Omega u_{ht}v^*dx = \frac{1}{2}B_A(u_h, v) + \int_\Omega \Phi(x)u_h v^*dx + \int_\Omega \mu|u_h|^{p-1}u_h v^*dx,$$

where

$$\begin{aligned}
B_A(u_h, v) = &\sum_{K\in\mathcal{T}_h}\int_K (\nabla u_h - 2\mathrm{i}Au_h)\cdot\nabla v + (|A|^2 - \mathrm{i}\nabla\cdot A)u_h v\, dx \\
&+ \sum_{e\in\Gamma_h^0}\int_e ((\beta h_e^{-1}[u_h] + \{\partial_n u_h\} - 2\mathrm{i}A\cdot n\{u_h\})[v] + [u_h]\{\partial_n v\})ds \\
&- \sum_{e\in\Gamma_h^\partial}\int_e ((\beta h_e^{-1}(0 - u_h) + \partial_n u_h - \mathrm{i}A\cdot nu_h)v + (u_h - 0)\partial_n v)ds.
\end{aligned}$$

Here, the boundary condition is weakly enforced in such a way that the boundary data are used whenever available; otherwise the trace of the numerical solution in corresponding boundary faces will be used.

Remark 3.2. Our analysis so far shows that for any parameter $\beta \in \mathbb{R}$, the DG scheme (2.4) preserves the two conservation properties. Moreover, the optimal convergence is ensured if $\beta > 0$ is sufficiently large. We should point out that in numerical simulations other choices of β can also lead to optimal convergence, as extensively tested in [17].

4. Time discretization. In this section, we present a second order Strang splitting method to solve ODE system (2.4), for which mass remains conserved.

From time $t = t_n$ to t_{n+1}, Schrödinger equation (1.1) is solved in three steps: we solve

$$(4.1) \qquad \mathrm{i}u_t = fu, \quad f = f(x, |u|) := \Phi(x) + \mu|u|^{p-1}$$

for a half time step, and then solve

$$(4.2) \qquad \mathrm{i}u_t = -\frac{1}{2}\Delta_A u$$

for one time step; we follow this by solving (4.1) for another half time step. Here we solve ODE (4.1) exactly and solve (4.2) by the DG method presented in section 2.

ALGORITHM 4.1. *The Strang splitting algorithm is as follows:*
Step 1: *Initialization:*

$$u_h^0(x) = u_0(x) \quad \forall x \in S,$$

where S is the set of all quadrature points from each element K_j,

$$S = \{x_j^\alpha \in K_j, \quad \alpha = 1, \ldots, Q; \ j = 1, \ldots, N\},$$

which is used in the algorithm's implementation.
Step 2: *Given values of u_h^n on S, the solution of ODE (4.1) after a half time step is given by*

$$(4.3) \qquad w = u_h^n \exp\left(-\mathrm{i}f(x, |u_h^n|)\Delta t/2\right) \quad on\ S.$$

Step 3: *Find $w_h \in V_h$, by the DG method*

$$(4.4) \qquad \mathrm{i} \int_\Omega \frac{w_h - w}{\Delta t/2} v^* dx = \frac{1}{2} B_A(w_h, v), \quad v \in V_h,$$

where $\int_\Omega wv^* dx$ is understood as its numerical integration using only values of wv on S.

   We then define

$$\tilde{w} = 2w_h - w \quad on \ S.$$

Step 4: *The solution of ODE* (4.1) *with initial data $\tilde{w}$ is further given by*

$$(4.5) \qquad u_h^{n+1} = \tilde{w} \exp\left(-\mathrm{i} f(x, |\tilde{w}|)\Delta t/2\right) \quad on \ S.$$

Return to Step 2.

   For this algorithm, we have the following result.

   THEOREM 4.1. *The fully discrete Strang splitting DG algorithm* (4.1) *satisfies the discrete mass conservation law,*

$$M[u_h^{n+1}] = M[u_h^n],$$

where the discrete mass is defined by

$$M[v] := \sum_{j=1}^N |K_j| \sum_{\alpha=1}^Q |v(x_j^\alpha)|^2.$$

   Proof. From (4.3) and (4.5) we see that

$$|u_h^n| = |w|, \ |\tilde{w}| = |u_h^{n+1}| \quad \text{on } S.$$

Hence

$$M[u_h^n] = M[w], \quad M[\tilde{w}] = M[u_h^{n+1}].$$

It suffices to show $M[w] = M[\tilde{w}]$ holds in Step 3. Take $v = w_h \in V_h$ in (4.4), and notice that $w_h = \frac{\tilde{w} + w}{2}$; then

$$\mathrm{i} \sum_{j=1}^N |K_j| \sum_{\alpha=1}^Q \frac{\tilde{w}(x_j^\alpha) - w(x_j^\alpha)}{\Delta t} \cdot \frac{\tilde{w}^*(x_j^\alpha) + w^*(x_j^\alpha)}{2} = \frac{1}{2} B_A(w_h, w_h). \qquad \square$$

Using (2.7), and upon separation of real and imaginary parts, we conclude

$$M[\tilde{w}] = M[w].$$

   Remark 4.1. One may also design a time-stepping scheme so that both mass and energy remain preserved. One option is that
(4.6)
$$\mathrm{i} \int_\Omega D_t u_h v^* dx = \frac{1}{2} B_A(u_h^{n+1/2}, v) + \int_\Omega \left(\Phi(x) + \int_0^1 g(\theta |u_h^{n+1}|^2 + (1-\theta)|u_h^n|^2)d\theta \right) u_h^{n+1/2} v^* dx.$$

Here

$$D_t u_h^n = \frac{u_h^{n+1} - u_h^n}{\tau}, \ u_h^{n+1/2} = (u_h^{n+1} + u_h^n)/2,$$

and $g(s) = \mu s^{(p-1)/2}$. Against testing function $v = u_h^{n+1/2}$ and $v = D_t u_h^n$, respectively, upon separation of real and imaginary parts, we obtain that

$$M_h^{n+1} = M_h^n, \quad E_h^{n+1} = E_h^n$$

for any $n \geq 0$, where $M_h^n = \int_\Omega |u_h^n|^2 dx$ and

$$E_h^n = \frac{1}{2} B_A(u_h^n, u_h^n) + \int_\Omega \left(\Phi|u_h^n|^2 + \int_0^{|u_h^n|^2} g(s)ds \right) dx.$$

Noting that (4.6) is nonlinear, we can update to get u_h^{n+1} the following way: find $w_h \in V_h$ by iteratively solving

$$\langle (i + \Phi(x) + \hat{g}_l)w_h^{l+1}, v \rangle - \frac{\tau}{4} B_A(w_h^{l+1}, v) = i\langle u_h^n, v \rangle \quad \forall v \in V_h,$$

where

$$\hat{g}_l := \int_0^1 g\left(\theta|2w_h^l - u_h^n|^2 + (1-\theta)|u_h^n|^2 \right) d\theta,$$

with $l = 0, 1, \ldots, L$, provided $\|w_h^L - w_h^{L-1}\| \leq \delta$, with some tolerance level δ; then

$$u_h^{n+1} = 2w_h - u_h^n.$$

We refer the reader to [9] for a recent study on this sort of time discretization for NLS equations without magnetic forces.

We also remark that, instead of using the formula

$$E_h(t) := \frac{1}{2} B_A(u_h, u_h) + \int_\Omega \left(\Phi|u_h|^2 + \frac{2\mu}{p+1}|u_h|^{p+1} \right) dx$$

as the discrete energy, one may use

$$\tilde{E}_h(t) := \frac{1}{2} \int_\Omega |q_h|^2 dx + \int_\Omega \left(\Phi|u_h|^2 + \frac{2\mu}{p+1}|u_h|^{p+1} \right) dx,$$

where $q_h \in V_h$ as an approximation to $\nabla u - iAu$ is determined by

$$\int_\Omega q_h v^* dx = - \sum_{K \in \mathcal{T}_h} (\langle u_h, \nabla \cdot v^* \rangle_K + i\langle Au_h, v \rangle_K) - \sum_{e \in \Gamma_h^0} \langle \{\partial_n u_h\}[v^*] \rangle_e$$

for the periodic case.

5. Numerical experiments. In this section, we present numerical examples to test the performance of the proposed schemes and verify our theoretical findings, based on the DG formulation (2.4) with (2.1). We use the Strang splitting method for NLS equations so that the method is both mass-preserving and second order in time.

The L^2 error is measured in discrete norm

$$\|v - v_h\| := \left(\sum_{\alpha=1}^N \sum_{i=1}^Q \omega_i(v(x_\alpha^i, t) - v_h(x_\alpha^i, t))^2 |K_\alpha| \right)^{1/2},$$

where $v = u^R$ or u^I, the real or imaginary part of u, and v_h is the corresponding part of the numerical solution. Here x_α^i is the ith quadrature point associated with weight ω_i so that $\sum_{i=1}^{Q} \omega_i = 1$. In our two-dimensional numerical tests, we take $Q = 25$ for all polynomial elements we tested. For the parameter β in numerical flux (2.1), we take $\beta = 4, 8, 20$ for $Q^k, k = 1, 2, 3$, approximations, respectively.

Unless otherwise pointed out, rectangle domains with periodic boundary conditions will be considered. In our numerical experiments, we take $A = 0$ and $\Phi(x_1, x_2) = \frac{1}{2} \sum_{j=1}^{2} \gamma_j x_j^2$ first, and then take nontrivial A to demonstrate the scheme performance in the presence of magnetic forces.

5.1. BEC simulations. We begin with an example to test the method accuracy and verify its mass-preserving feature in long time simulations.

Example 5.1. *We solve the two-dimensional NLS equation*

$$\mathrm{i}u_t = -\frac{1}{2}\Delta u + \Phi u + |u|^2 u, \quad x \in [0, 2\pi]^2,$$

with periodic boundary condition and initial data

$$u(x, y, 0) = e^{\mathrm{i}(x+y)}.$$

When taking $\Phi(x, y) = -4$, the exact solution is a plane wave solution

$$u(x, y, t) = e^{\mathrm{i}(x+y+2t)}.$$

We test this example using the $Q^k, k = 1, 2, 3$, polynomial elements on a uniform mesh with $N \times N$ cells. In Table 1, we list the L^2 errors and orders of accuracy of Q^k approximations, respectively. We see that the optimal $k + 1$ order of accuracy is achieved for Q^k approximation. To verify the conservative property of the DG method, we carry out the computation up to $t = 20$ with Q^2 approximation and $\Delta t = 0.001$. Figure 1 plots the history of the relative mass $\frac{M_h(t)}{M_h(0)}$ and relative energy $\frac{\tilde{E}_h(t)}{\tilde{E}_h(0)}$, respectively. It shows that the mass $M_h(t)$ and energy $\tilde{E}_h(t)$ are preserved.

TABLE 1
Errors for Example 5.1 when using $Q^k, k = 1, 2, 3$, polynomials on a uniform mesh of $N \times N$ cells. Final time is $T = 1$.

Q^k	N	Δt	$\|u^R - u_h^R\|$	Order	$\|u^I - u_h^I\|$	Order
	10	2.0e-02	6.9182e-01	-	6.9182e-01	-
	20	1.0e-02	1.8460e-01	1.91	1.8460e-01	1.91
$k = 1$	40	5.0e-03	4.6623e-02	1.99	4.6623e-02	1.99
	80	2.5e-03	1.1761e-02	1.99	1.1761e-02	1.99
	160	1.25e-03	2.9611e-03	1.99	2.9611e-03	1.99
	10	2.0e-02	6.1087e-03	-	6.1087e-03	-
	20	5.0e-03	6.1798e-04	3.31	6.1798e-04	3.31
$k = 2$	40	1.25e-03	7.7198e-05	3.00	7.7198e-05	3.00
	80	3.125e-04	1.2356e-05	2.64	1.2356e-05	2.64
	160	7.8125e-05	1.3115e-06	3.24	1.3115e-06	3.24
	10	4.0e-02	7.7716e-04	-	7.7716e-04	-
	20	1.0e-02	4.6005e-05	4.08	4.6005e-05	4.08
$k = 3$	40	2.5e-03	2.7499e-06	4.06	2.7499e-06	4.06
	80	6.25e-04	1.9810e-07	3.80	1.9810e-07	3.80
	160	1.5625e-04	1.1840e-08	4.06	1.1841e-08	4.06

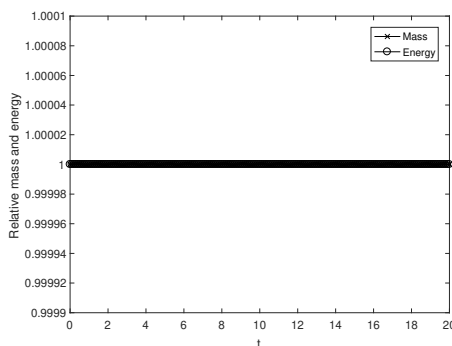In the following, we test the method's performance using examples for the BEC simulation.

FIG. 1. *Example* 5.1. *Mass and energy history.*

Example 5.2. We solve the two-dimensional NLS equation

$$\mathrm{i}u_t = -\frac{1}{2}\Delta u + \Phi u + \mu|u|^2 u$$

over $\Omega = [-8,8]^2$ with periodic boundary condition. This corresponds to (1.1) with $A = 0$ and $p = 3$. The parameter μ is either positive (repulsive) or negative (attractive), with potential of form

$$\Phi = \frac{1}{2}(\gamma_1 x^2 + \gamma_2 y^2).$$

Defocusing case. With $\mu = 1$ and initial data taken as a Gaussian,

(5.1) $$u_0(x,y) = \frac{1}{\sqrt{\pi}}e^{-\frac{x^2+y^2}{2}},$$

we carry out the numerical simulation on the uniform mesh with 256×256 cells and time step $\Delta t = 0.01$. Figure 2 plots the numerical mode $|u(x,y,t)|$ at different times with different potentials:
(i) $\Phi = (x^2 + 4y^2)/2$ is attracting and confines waves to the ground state,
(ii) $\Phi = (x^2 - y^2)/2$ enhances the dispersion, and
(iii) $\Phi = (-x^2 - y^2)/2$ shows dispersion in both x and y directions.
These numerical results are in agreement with those reported in [10]. We can see clearly that attractive Φ confines the waves to the ground state, while the repulsive Φ enhances the dispersion or scattering.
Focusing case. Consider

$$\mathrm{i}\varepsilon u_t = -\frac{1}{2}\varepsilon^2 \Delta u + \Phi u + \mu|u|^2 u,$$

with potential of form

$$\Phi = \frac{1}{2\varepsilon}(\gamma_1 x^2 + \gamma_2 y^2)$$

and initial data

$$u_0(x,y) = \frac{1}{\sqrt{\varepsilon\pi}}e^{-\frac{x^2+y^2}{2\varepsilon}}.$$

The focusing case with $\mu = -1.9718 < 0$ and $\varepsilon = 0.3$ has also been studied in [10]. In such a case, the focusing NLS equation can have finite blowup solutions. The
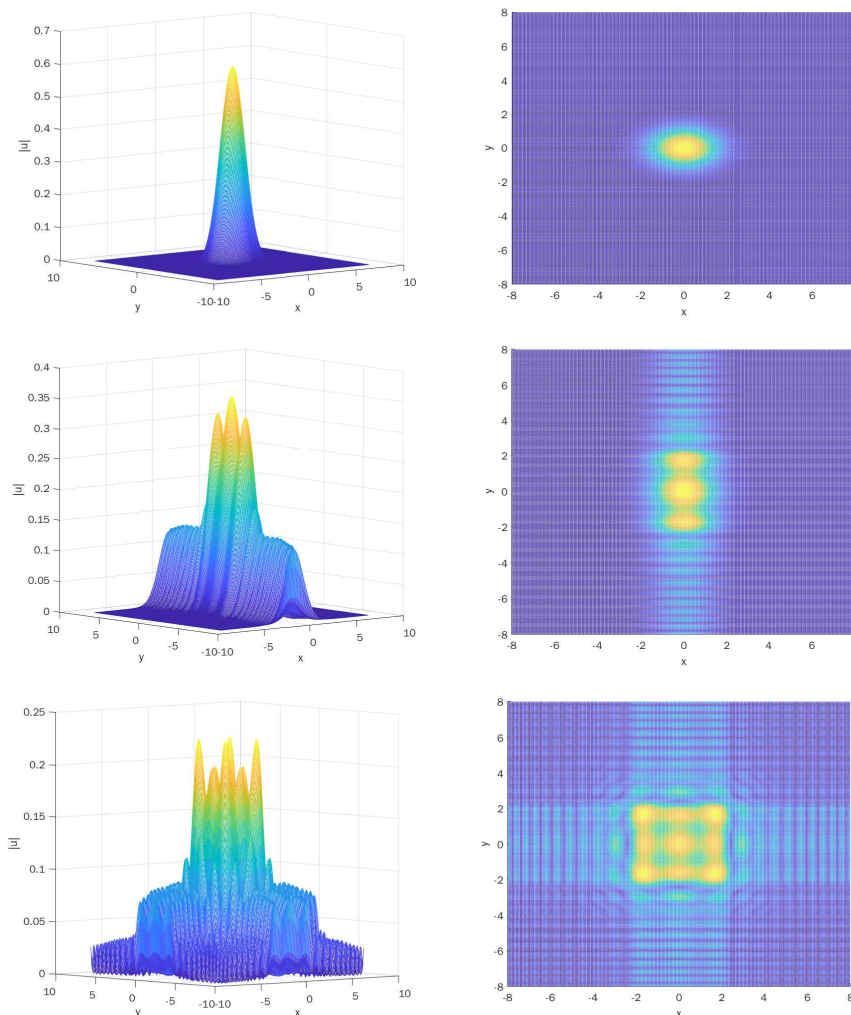
FIG. 2. *Example* 5.2. *Defocusing* $\mu = 1$, $\varepsilon = 1$, *numerical* $|u(x,y,t)|$. *Left: 3D view of* $|u(x,y,t)|$. *Right: Top view of* $|u(x,y,t)|$. *Top:* $\Phi = (x^2 + 4y^2)/2$, $t = 2.0$. *Middle:* $\Phi = (x^2 - y^2)/2$, $t = 5.0$. *Bottom:* $\Phi = (-x^2 - y^2)/2$, $t = 5.0$.

attractive potential Φ confines the cooled bosonic atoms, and the repulsive potential Φ supports the dispersion. Numerical simulations are carried out using a uniform mesh with 256×256 cells and time step $\Delta t = 0.001$. Figure 3 plots the numerical amplitude $\max |u(x,y,t)|, t \in [0,1]$. A blowup time of approximately 0.3 seconds is observed when $\Phi = \frac{x^2 + y^2}{2\varepsilon}$, and the blowup time has been delayed slightly when $\Phi = -\frac{x^2 + y^2}{2\varepsilon}$. We observe wild oscillations after the blowup time.

5.2. Magnetic effects. Consider the BEC with rotation, or more generally the NLS equation subjected to magnetic fields [1, 22, 38]. It would be interesting to see how the excited states are formed and how dispersion or scattering can be achieved by appropriately manipulating BEC with potentials and magnetic fields.
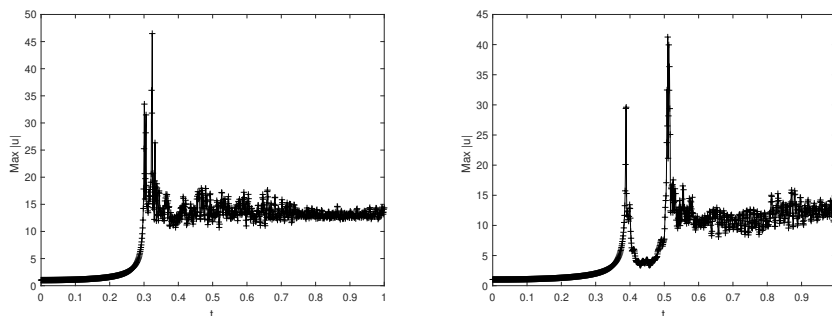
FIG. 3. *Example* 5.2. *Focusing* $\mu = -1.9718$, $\varepsilon = 0.3$, *numerical* $\max_{(x,y)\in\Omega} |u(x,y,t)|$. *Left:* $\Phi = \frac{x^2+y^2}{2\varepsilon}$. *Right:* $\Phi = -\frac{x^2+y^2}{2\varepsilon}$.

Our numerical experiments considered the linear Schrödinger equation

(5.2) $$iu_t = -\frac{1}{2}(\nabla - iA)^2 u + \Phi u,$$

with different potentials A and Φ.

Example 5.3. In this example, we solve (5.2) over computational domain $[0,1]^2$,

$$A_1(x,y) = \sin(2\pi y), \quad A_2(x,y) = \sin(2\pi x),$$

$$\Phi(x,y) = -1 - 4\pi^2 + 2\pi(A_1 + A_2) - \frac{1}{2}\left(A_1^2 + A_2^2\right),$$

and initial value

$$u_0(x,y) = e^{i2\pi(x+y)}.$$

The corresponding exact solution is

$$u(x,y,t) = e^{i(2\pi(x+y)+t)}.$$

We first test the accuracy and convergence rate using the Q^k polynomials with $k = 1, 2, 3$ on a uniform mesh with $N \times N$ cells. Table 2 reports the L^2 errors and orders of accuracy. We observe that the DG method achieves the optimal $k+1$ order for even $k = 1, 2, 3$. We then test the conservation property of the scheme using Q^2 polynomials and $\Delta t = 0.01$. Figure 4 plots the history of the relative mass $\frac{M_h(t)}{M_h(0)}$ and energy $\frac{\tilde{E}_h(t)}{\tilde{E}_h(0)}$, respectively. It shows that the mass $M_h(t)$ and energy $\tilde{E}_h(t)$ are preserved well during the simulation up to $t = 20$.

Example 5.4. We solve (5.2) in the two-dimensional setting, over interval $[-5,5]^2$,

$$A_1(x,y) = -3\sin\left(\frac{2\pi(y+5)}{10}\right), \quad A_2(x,y) = 3\sin\left(\frac{2\pi(x+5)}{10}\right),$$

$$\Phi(x,y) = 20\cos\left(\frac{2\pi(x+5)}{10}\right) + 20\cos\left(\frac{2\pi(y+5)}{10}\right) + 40,$$

and initial data

$$u_0(x,y) = \sqrt{\frac{\sqrt{10}}{\pi}} \exp\left(-\frac{\sqrt{10}}{2}((x-1)^2 + y^2)\right).$$

This numerical example was tested in [6] using a splitting approach.

TABLE 2
Errors for Example 5.3 *when using* $Q^k, k = 1, 2, 3$, *polynomials on a uniform mesh of* $N \times N$
cells. Final time is $T = 1$.

| Q^k	N	Δt	$\|u^R - u_h^R\|$	Order	$\|u^I - u_h^I\|$	Order
	20	2.0e-03	8.2110e-01	-	8.2117e-01	-
$k=1$	40	1.0e-03	2.2304e-01	1.88	2.2395e-01	1.87
	80	5.0e-04	5.6289e-02	1.99	5.6289e-02	1.99
	160	2.5e-04	1.4095e-02	2.00	1.4087e-02	2.00
	10	1.0e-03	2.3364e-03	-	2.4825e-03	-
$k=2$	20	2.5e-04	1.8422e-04	3.66	1.9191e-04	3.69
	40	6.25e-04	1.7261e-05	3.42	1.7576e-05	3.45
	80	1.5625e-05	1.9155e-06	3.17	2.1364e-06	3.04
	10	1.0e-03	3.9507e-03	-	4.1111e-03	-
$k=3$	20	2.5e-04	2.4776e-04	4.00	2.5775e-04	4.00
	40	6.25e-05	1.5495e-05	4.00	1.6131e-05	4.00
	80	1.5625e-05	1.0121e-06	3.94	1.0330e-06	3.97
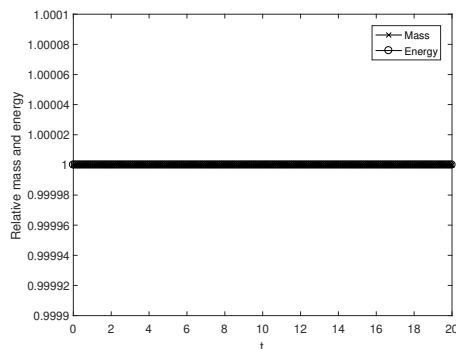
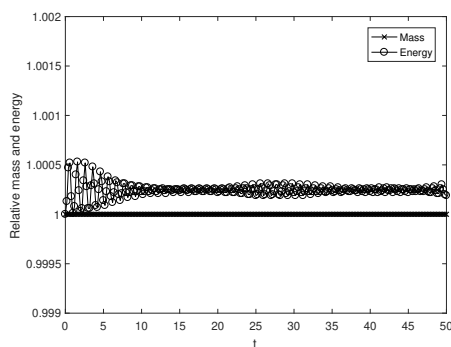
FIG. 4. *Example* 5.3. *Mass and energy history.*

FIG. 5. *Example* 5.4. *Mass and energy history.*

The final time $T = 50$ and time step $\Delta t = 0.01$. Figure 5 plots the history of
the relative mass $\frac{M_h(t)}{M_h(0)}$ and relative energy $\frac{\tilde{E}_h(t)}{\tilde{E}_h(0)}$. We observe that, for this long-
term simulation, the mass is well preserved by the DG method, and the energy is
asymptotically preserved as the discrete energy appears to evolve quite close to the
initial energy.

6. Concluding remarks. In this paper, we construct and analyze a high-order DG method for the nonlinear Schrödinger equation in the presence of an electromagnetic field. The semidiscrete scheme is shown to preserve both mass and energy. Optimal L^2 error estimates are obtained in the full nonlinear setting. For time discretization, we use the second order Strang splitting method to solve the nonlinear Schrödinger equation. We perform a number of numerical tests showing that the method is both accurate and robust, and both mass and energy are well preserved over long time simulation. Therefore, it can be considered as a competitive algorithm in the solution of the nonlinear Schrödinger equation.

REFERENCES

[1] P. Antonelli, D. Marahrens, and C. Sparber, *On the Cauchy problem for nonlinear Schrödinger equations with rotation*, Discrete Contin. Dyn. Syst., 32 (2012), pp. 703–715.
[2] D. N. Arnold, *An interior penalty finite element method with discontinuous elements*, SIAM J. Numer. Anal., 19 (1982), pp. 742–760, https://doi.org/10.1137/0719052.
[3] D. N. Arnold, F. Brezzi, B. Cockburn, and L. D. Marini, *Unified analysis of discontinuous Galerkin methods for elliptic problems*, SIAM J. Numer. Anal., 39 (2002), pp. 1749–1779, https://doi.org/10.1137/S0036142901384162.
[4] W. Z. Bao, S. Jin, and P. A. Markowich, *On time-splitting spectral approximations for the Schrödinger equation in the semiclassical regime*, J. Comput. Phys., 175 (2002), pp. 487–524.
[5] J. Bona, H. Chen, O. Karakashian, and Y. Xing, *Conservative, discontinuous Galerkin–methods for the generalized Korteweg–de Vries equation*, Math. Comp., 82 (2013), pp. 1401–1432.
[6] M. Caliari, A. Ostermann, and C. Piazzola, *A splitting approach for the magnetic Schrödinger equation*, J. Comput. Appl. Math., 316 (2017), pp. 74–85.
[7] P. G. Ciarlet, *The Finite Element Method for Elliptic Problems*, Stud. Math. Appl. 4, North-Holland, Amsterdam, 1978.
[8] A. de Bouard, *Nonlinear Schrödinger equations with magnetic fields*, Differential Integral Equations, 4 (1991), pp. 73–88.
[9] X. Feng, H. Liu, and S. Ma, *Mass- and energy-conserved numerical schemes for nonlinear Schrödinger equations*, Commun. Comput. Phys., 26 (2019), pp. 1365–1396.
[10] L. Galati and S. Zheng, *Nonlinear Schrödinger equations for Bose-Einstein condensates*, AIP Conf. Proc., 50 (2013), 1562.
[11] V. Gradinaru, *Strang splitting for the time dependent Schrödinger equation on sparse grids*, SIAM J. Numer. Anal., 46 (2007), pp. 103–123, https://doi.org/10.1137/050629823.
[12] J. S. Hesthaven and T. Warburton, *Nodal Discontinuous Galerkin Methods: Algorithms, Analysis, and Applications*, Springer, New York, 2007.
[13] J. Hong, L. Ji, and Z. Liu, *Optimal error estimates of conservative local discontinuous Galerkin method for nonlinear Schrödinger equation*, Appl. Numer. Math., 127 (2018), pp. 164–178.
[14] S. Jin and Z. Zhou, *A semi-Lagrangian time splitting method for the Schrödinger equation with vector potentials*, Commun. Inf. Syst., 13 (2013), pp. 247–289.
[15] X. Liang, A. Khaliq, and Y. Xing, *Fourth order exponential time differencing method with local discontinuous Galerkin approximation for coupled nonlinear Schrödinger equations*, Commun. Comput. Phys., 17 (2015), pp. 510–541.
[16] H. Liu, *Optimal error estimates of the direct discontinuous Galerkin method for convection-diffusion equations*, Math. Comp., 84 (2015), pp. 2263–2295.
[17] H. Liu, Y.-Q. Huang, W.-Y. Lu, and N.-Y. Yi, *On accuracy of the mass preserving DG method to multi-dimensional Schrödinger equations*, IMA J. Numer. Anal., 39 (2019), pp. 760–791.
[18] H. Liu and N. Ploymaklam, *A local discontinuous Galerkin method for the Burgers-Poisson equation*, Numer. Math. 129 (2015), pp. 321–351.
[19] H. Liu and N.-Y. Yi, *A Hamiltonian preserving discontinuous Galerkin method for the generalized Korteweg-de Vries equation*, J. Comput. Phys., 326 (2017), pp. 776–796.
[20] H. Liu and J. Yan, *The direct discontinuous Galerkin (DDG) methods for diffusion problems*, SIAM J. Numer. Anal., 47 (2009), pp. 675–698, https://doi.org/10.1137/080720255.

[21] H. Liu and J. Yan, *The Direct Discontinuous Galerkin (DDG) method for diffusion with interface corrections*, Commun. Comput. Phys., 8 (2010), pp. 541–564.

[22] H. Liu and E. Tadmor, *Rotation prevents finite-time breakdown*, Phys. D, 188 (2004), pp. 262–276.

[23] J. Lu and J. Marzuola, *Strang splitting methods applied to a quasilinear Schrödinger equation: Convergence, instability, and dynamics*, Commun. Math. Sci., 13 (2015), pp. 1051–1074.

[24] T. Lu, W. Cai, and P. W. Zhang, *Conservative local discontinuous Galerkin methods for time dependent Schrödinger equation*, Int. J. Numer. Anal. Model., 2 (2005), pp. 75–84.

[25] W.-Y. Lu, Y.-Q. Huang, and H. Liu, *Mass preserving direct discontinuous Galerkin methods for Schrödinger equations*, J. Comput. Phys., 282 (2015), pp. 210–226.

[26] C. Lubich, *On splitting methods for Schrödinger–Poisson and cubic nonlinear Schrödinger equations*, Math. Comp., 77 (2008), pp. 2141–2153.

[27] L. Michel, *Remarks on non-linear Schrödinger equation with magnetic fields*, Comm. Partial Differential Equations, 33 (2008), pp. 1198–1215.

[28] Y. Nakamura, *Local solvability and smoothing effects of nonlinear Schrödinger equations with magnetic fields*, Funkcial. Ekvac., 44 (2001), pp. 1–18.

[29] L. Pitaevskii, *Vortex lines in an imperfect Bose gas*, Soviet. Phys. JETP, 13 (1961), pp. 451–454.

[30] B. Rivière, *Discontinuous Galerkin Methods for Solving Elliptic and Parabolic Equations: Theory and Implementation*, Frontiers Appl. Math. 35, SIAM, Philadelphia, 2008, https://doi.org/10.1137/1.9780898717440.

[31] C.-W. Shu, *Discontinuous Galerkin methods: General approach and stability*, in Numerical Solutions of Partial Differential Equations, S. Bertoluzza, S. Falletta, G. Russo, and C.-W. Shu, eds., Adv. Courses Math. CRM Barcelona, Birkhäuser, Basel, 2009, pp. 149–201.

[32] G. Strang, *On the construction and comparison of difference schemes*, SIAM J. Numer. Anal., 5 (1968), pp. 506–517, https://doi.org/10.1137/0705041.

[33] Y. Xu and C.-W. Shu, *Local discontinuous Galerkin methods for nonlinear Schrödinger equations*, J. Comput. Phys., 205 (2005), pp. 72–97.

[34] Y. Xu and C.-W. Shu, *Optimal error estimates of the semidiscrete local discontinuous Galerkin methods for high order wave equations*, SIAM. J. Numer. Anal., 50 (2012), pp. 79–104, https://doi.org/10.1137/11082258X.

[35] R. P. Zhang, X. J. Yu, and T. Feng, *Solving coupled nonlinear Schrödinger equations via a direct discontinuous Galerkin method*, Chinese Phys. B, 21 (2012), 30202.

[36] R. Zhang, X. Yu, M. Li, and X. Li, *A conservative local discontinuous Galerkin method for the solution of nonlinear Schrödinger equation in two dimensions*, Sci. China Math., 60 (2017), pp. 2515–2530.

[37] R. P. Zhang, X. J. Yu, and G. Z. Zhao, *A direct discontinuous Galerkin method for nonlinear Schrödinger equation*, Chinese J. Comput. Phys., 29 (2012), pp. 175–182 (in Chinese).

[38] S. Zheng, *Fractional regularity for nonlinear Schrödinger equations with magnetic fields*, Contemp. Math., 581 (2012), pp. 271–285.